Systematic *ab initio* study of the electronic and magnetic properties of different pure and mixed iron systems

J. Izquierdo, A. Vega, and L. C. Balbás
Departamento de Física Teórica, Universidad de Valladolid, E-47011 Valladolid, Spain

Daniel Sánchez-Portal
Department of Physics and Materials Research Laboratory, University of Illinois, Urbana, Illinois 61801

Javier Junquera and Emilio Artacho
Departamento de Física de la Materia Condensada, C-III, and Institut Nicolás Cabrera, Universidad Autónoma de Madrid, 28049 Madrid, Spain

Jose M. Soler
Department of Physics, Harvard University, Cambridge, Massachusetts 02138

Pablo Ordejón
Institut de Ciència de Materials de Barcelona (CSIC), Campus de la U.A.B., Bellaterra, E-08193 Barcelona, Spain
(Received 26 October 1999; revised manuscript received 8 February 2000)

We present a theoretical study of the electronic and magnetic properties of iron systems in different environments: pure iron systems [dimer, bcc bulk, (100) surface, and free-standing iron monolayer], and low-dimensional iron systems deposited on Ag (100) surface (monoatomic linear wires, iron monolayer, planar, and three-dimensional clusters). Electronic and magnetic properties have been calculated using a recently developed total-energy first-principles method based on density-functional theory with numerical atomic orbitals as a basis set for the description of valence electrons and nonlocal pseudopotentials for the atomic core. The Kohn-Sham equations are solved self-consistently within the generalized gradient approximation for the exchange-correlation potential. Tests on the pseudopotential, the basis set, grid spacing, and k sampling are carefully performed. This technique, which has been proved to be very efficient for large nonmagnetic systems, is applied in this paper to calculate electronic and magnetic properties of different iron nanostructures. The results compare well with previous *ab initio* all-electron calculations and with experimental data. The method predicts the correct trends in the magnetic moments of Fe systems for a great variety of environments and requires a smaller computational effort than other *ab initio* methods.

I. INTRODUCTION

Low-dimensional magnetic systems constitute one of the key ingredients in the development of new storage devices characterized by high storage density and miniaturization.[1] The interest of the scientific community in low-dimensional magnetic systems from both the fundamental and practical points of view is not new and started after the discovery of the possibility of enhancing the magnetic moment of a material by diminishing the atomic coordination.[2] In this context, it is well known that the surfaces and free-standing clusters of ferromagnets display a larger magnetic moment per atom than in the bulk configuration and that free clusters of certain paramagnetic materials like Rh or V are magnetic.[1,3] A great impulse in the study of low-dimensional magnetism, from both experiment and theory, was given by the discovery of the magnetoresistance in Fe/Cr and other multilayers.[4] This opened new prospects in materials science: for instance, one of the current goals is to obtain two-dimensional magnetoresistive materials by depositing atomic wires on a surface.

In contrast to the great improvement in the experimental techniques for growing and characterizing low-dimensional magnetic systems, particularly when they are supported on a substrate, the theoretical models have limitations in several respects. Usual *ab initio* methods, either all electron full potential linear augmented-plane-wave [(FLAPW) (Ref. 5), Korringa-Kohn-Rostoker (KKR) (Ref. 6), linear muffin tin orbital (LMTO) (Ref. 7)] or based on pseudopotentials for describing the effect of the core electrons,[8] are designed to deal with periodic structures. Their formulation in k space requires using supercells for nonperiodic systems and this, particularly with delocalized basis, makes them prohibitive for realistic systems of low symmetry. However, it is desirable to retain the high accuracy of those first-principle methods.

On the other side, semiempirical model Hamiltonians have been proposed to overcome the difficulties related to low symmetry and large system sizes.[9] These methods are formulated in real space and use localized bases so that nonperiodic systems without symmetry are easy to deal with. In the particular case of magnetic systems, the self-consistent tight-binding model has been successfully applied for the study of free[9] and supported clusters,[10] surfaces, and overlayers.[11] However, a good parametrization has to be found and, although this is possible through fittings to *ab*

initio results for simple systems, its degree of transferability is better for certain materials than for others.

For the study of low-dimensional magnetic systems, we use in this paper a numerical linear combination of atomic orbitals density functional theory (LCAO DFT) approach that has been recently developed and designed for efficient calculations in large and low-symmetry systems. It has been applied successfully to quite varied systems, ranging from metal nanostructures to biomolecules, showing accuracy and flexibility. We have used the SIESTA code,[12–16] which performs a fully self-consistent density functional (DFT) calculation to solve the standard Kohn-Sham equations[17] in the local or gradient-corrected (spin) density approximations [local density approximation (LDA)/local spin density approximation (LSDA)/generalized-gradient approximation (GGA)][18,19] using a linear combination of numerical atomic orbitals as the basis set, and standard norm-conserving pseudopotentials[20] in their fully nonlocal form.[21] More details on the method are given in Sec. II below.

Our aim in this paper is to demonstrate the applicability of the method to the study of low-dimensional magnetic systems and for this purpose we have chosen iron-based systems. The reason of this choice is double. On one hand, iron-based systems have been widely investigated through both all electron *ab initio* methods and semiempirical methods so that we can compare our results. On the other hand, it is an element of great current interest; maybe it is also the most studied magnetic element experimentally and it is not completely understood so far in many respects.

We have organized the paper as follows. The theoretical method is presented in the next section. The different approximations are analyzed, in particular, the choice of the nonlocal pseudopotential and the basis set. In Sec. III we study pure iron systems: the dimer, the bulk, a (100) surface, and a (100) free-standing monolayer. In this way we test the transferability of our Fe pseudopotential and basis set. The cohesive energy, bond length, vibrational frequency, and spin polarization of the free Fe dimer are calculated using different basis sets, and the results are compared to experiments and to other calculations. The results for the spin-polarized band structure of bcc Fe is calculated and values for the magnetic moment, density of states, exchange splitting, and electronic occupation are discussed and compared with other *ab initio* results and with experiments. Also, the magnetic moments of the (100) surface and free-standing monolayer are calculated, showing good agreement with previous calculations. These calculations show that the method is able to deal with a wide variety of iron systems using the same pseudopotential and basis set. Section IV is devoted to low-dimensional Fe systems supported on Ag(100): clusters with linear (wires), planar, and three-dimensional configurations are studied as typical examples of supported nanostructures. We analyze the influence of different chemical environments through the hybridization and interface effects. The main conclusions of this work are summarized in the last section, together with the perspectives for the future, particularly in connection with molecular-dynamics simulation and noncollinear magnetism.

II. THEORETICAL MODEL

In this section we describe briefly the numerical-LCAO DFT computational scheme,[12–16] as implemented in the SIESTA code. Details about the choice of the pseudopotential, basis set, and computational parameters are also given. The method is based on DFT, using both local-density[17,18] and generalized-gradients functionals,[19] including spin polarization, both collinear and noncollinear.[22] Core electrons are replaced by norm-conserving pseudopotentials[20] factorized in the Kleinman-Bylander form,[21] including scalar-relativistic effects, and nonlinear partial-core corrections.[23] The one-particle problem is then solved using a LCAO of (pseudo) atomic orbitals (PAO's). The main advantage of atomic orbitals is their efficiency (fewer orbitals needed per electron for similar precision) and their main disadvantage is the lack of systematics for optimal convergence, a well-known issue in quantum chemistry.[24] In our approach, there are no constraints either on the radial shape of these numerical orbitals or on the size of the basis, allowing for the full quantum-chemistry know-how[25] (multiple-ζ, polarization, off-site, contracted, and diffuse orbitals). In order to limit the range of the pseudoatomic basis orbitals, they are slightly excited by a common ''energy shift'' δE_{PAO}, and truncated at the resulting radial node.[26] Schemes to generate multiple-ζ and polarization orbitals within finite truncation ranges were also developed, as described elsewhere.[15] These basis orbitals are projected on a uniform grid in real space to calculate the density, the Hartree and exchange-correlation potentials, and the local part of the pseudopotential. The same grid is used to calculate the matrix elements of the self-consistent potential between basis orbitals.

The basis functions and the electron density are projected onto a uniform real-space grid in order to calculate the Hartree and exchange-correlation potentials and matrix elements. Given the Hamiltonian, the one-particle Schrödinger equation is solved yielding the energy and density matrix for the ground state. This task is performed either by diagonalization (cube-scaling, appropriate for systems under 100 atoms or for metals) or with a linear-scaling algorithm. These have been extensively reviewed elsewhere.[27] In this work we use a standard diagonalization method to solve the secular matrix problem, because of the difficulty of linear-scaling algorithms to treat metallic systems.[27] From the resulting density matrix, a new Hamiltonian matrix is obtained in $O(N)$ operations, and the self-consistency loop is iterated to convergence.

In our simulations, we use soft ionic pseudopotentials generated according to the procedure of Troullier and Martins[20] from the atomic configurations $[\mathrm{Ar}]3d^7 4s^1$ for Fe and $[\mathrm{Kr}]4d^{10}5s^1$ for Ag. The core radii for the *s*, *p*, and *d* components in Fe are all 2.00 a.u., and in Ag, 2.60, 2.80, and 2.60 a.u., respectively. A weighted average of the scalar relativistic potentials is used both for Fe and Ag. Up to *f* angular momentum components of the nonlocal pseudopotential are treated via the Kleinman-Bylander construction,[21] while the local part is optimized for smoothness.

Due to the well-known failure of LSDA to predict the bcc ground state of bulk iron, we use the GGA for the exchange-correlation potential as parametrized by Perdew, Burke, and Ernzerhof.[19] The calculation of density gradients is performed numerically[28] (with a five-point Lagrange interpolation) for the discrete set of grid points. The partial-core correction for nonlinear exchange correlation[23] has been included. A careful study of the optimum core correction

TABLE I. Properties of Fe_2 obtained with the SIESTA code. We use the GGA, an integration grid cutoff of 150 Ry, and a basis-orbital energy shift of 0.001 Ry for both SZSP and DZSP basis. The total spin in all the cases is $S=3\hbar$. Bond lengths r_e (bohrs), binding energies E_b (eV/atom), and vibrational frequencies ω_e (cm^{-1}) are shown. The binding energies E_b are calculated with respect to spherical ^5D Fe atoms. Other calculations and experimental results are given for comparison.

	SZSP	DZSP	PW-LSDA [a]	GTO-LSDA [b]	GTO-GGA [b]	Expt. [c]
r_e (bohrs)	3.88	3.76	3.71	3.71	3.78	(3.53, [c]3.82 [d])
E_b (eV/at)	1.35	1.55	2.06	2.19	1.62	(0.57, [e]0.65 [f])
$w_e(cm^{-1})$	341	370	453	418	474	300 [g]

[a]Reference 22.
[b]Reference 31.
[c]Reference 32.
[d]Reference 33.
[e]Reference 34.
[f]Reference 35.
[g]Reference 36.

radius for the Fe pseudopotential leads to a value of 0.7 a.u.

Two different basis sets were used for the present work to describe the valence states. The first one is a single-ζ set (containing one *s* orbital and five *d* orbitals), in which the *s* orbital was polarized by introducing a single shell of *p* orbitals. We will refer to this set as the single-ζ singly-polarized (SZSP) set. The second one is a double-ζ set, in which the *s* and *d* orbitals were doubled, and the *s* shell was also polarized with a single *p* shell. We refer to this second set as the double-ζ singly-polarized (DZSP) set. The grid fineness is controlled by the ''energy cutoff'' E_{cut} of the plane waves (PW) that can be represented in it without aliasing.[29] As a rough estimate, one can associate a grid spacing *h* with a PW cutoff of $(\pi/h)^2$ Ry with *h* in a.u. We have used an energy cutoff of 150 Ry, after checking that the results for bulk iron and for the iron dimer do not change significantly with increasing the energy cutoff up to 200 Ry.

The orbital contribution to the magnetic moment is neglected for all the Fe systems considered in this work, as in the previous calculations that we compare with. For bulk bcc Fe, the orbital contribution to the magnetic moment is small (about $0.08\mu_B$) and for free-standing clusters with a few dozens of atoms, that contribution is experimentally found to be about $0.1–0.2\mu_B$ with the total magnetic moment about $3\mu_B$ per atom.[2]

III. RESULTS FOR PURE IRON SYSTEMS

A. Iron dimer

The simulations for Fe_2 have been carried out with $\delta E_{PAO}=0.001$ Ry for both the SZSP and DZSP calculations. Table I shows our results for the spectroscopic properties of Fe_2 with total spin $S=3\hbar$, which corresponds to the experimental configuration ($^7\Delta_u$) and also to the ground state for the Fe dimer in our calculations. Let us point out here that if we generate the iron pseudopotential from the atomic configuration $[Ar]3d^64s^2$ instead of the used $[Ar]3d^74s^1$, we obtain $S=4\hbar$ for the equilibrium state of Fe_2, instead of the experimental value $S=3\hbar$.

Three previous calculations are also given in Table I; one of them[22] is taken from a recent PW calculation using the ultrasoft Vanderbilt pseudopotential[30] and the LSDA of Perdew and Zunger;[18] the two other sets of results come from an all-electron calculation[31] using a linear combination of Gaussian orbitals, the first with the LSDA of Vosko, Wilk, and Nusair,[37] and the second with the GGA of Perdew and Wang.[38] Experimental values obtained by different groups[32–36] are also given. We can see that the bond lengths and binding energies calculated within GGA are larger and smaller, respectively, than the corresponding LSDA values. In all the calculations, the binding energy E_b is calculated relative to the isolated spherical ^5D Fe atoms. A discussion of the improvement of the binding energy of Fe_2 when calculated relative to nonspherical atoms is given in the work of Castro and Salahub.[31] With respect to our results, we stress that despite the fact that the SZSP E_b is closer to experiments than the DZSP value, the DZSP solution is energetically more stable (and closer to the results converged with respect to the basis set).

We conclude by comparing the different results in Table I, that the pseudopotential of Fe used in our calculations in combination with the DZSP basis leads to results comparable to other standard high-quality *ab initio* calculations. The SZSP basis, although very small, also provides a very acceptable description of the dimer.

B. Fe bulk

It is well known that bulk iron is bcc, and that the GGA is needed to find the bcc structure as the ground state in *ab initio* calculations.[39–43] We have calculated bulk bcc Fe with both SZSP and DZSP basis sets. First of all we performed a study in order to find the cutoff radius for the pseudo-orbitals that minimizes the energy of the system. For both SZSP and DZSP basis sets, we obtain a cutoff radius of 4.90 a.u. for both the *s* and *d* orbitals. These basis sets and cutoff radii will be used later for more complicated Fe systems. The electron spin density and total energy are obtained from the wave functions calculated at 500 *k* points. No significant changes are found with up to 5000 *k* points.

In Table II we compare our results for the lattice parameter, bulk modulus, and magnetic moment (obtained with both the SZSP and DZSP basis) with results from other types of *ab initio* GGA calculations, either using pseudopotentials[44,45] or all electron,[42,39,43] as well as with the experimental values.[46] The different GGA's used in the previous calculations quoted in Table II are as follows. The GGA functional of Perdew and Wang[38] was used in the pseudopotential planewave PW,[44] the all-electron Gaussian

TABLE II. Convergence tests for bulk bcc iron using SZSP and DZSP basis. Lattice parameter a (bohrs), bulk modulus B (Mbar), and magnetic moment M (μ_B) are presented. Other *ab initio* calculations and experimental results are given for comparison.

	SZSP	DZSP	PW [a]	LAPW [b]	GTO [c]	FP-LMTO [d]	FLAPW [e]	Expt. [f]
a (bohrs)	5.44	5.44	5.60	5.40	5.44	5.43	5.44	5.42
B (Mbar)	2.32	1.90	1.45	1.69	1.74	1.60	1.82	1.68
$M(\mu_B)$	2.35	2.35	2.35	2.32	2.20	2.20	2.13	2.22

[a]Reference 44.
[b]Reference 45.
[c]Reference 42.
[d]Reference 39.
[e]Reference 43.
[f]Reference 46.

Type Orbitals GTO,[42] and the FLAPW calculations.[43] The GGA functional of Perdew[47] was used in the pseudopotential linear-augmented-plane-wave[45] (LAPW) and in the all-electron full-potential linear muffin-tin orbitals (FP-LMTO) calculation.[39] Our values for the lattice parameter of bulk Fe are in good agreement with the experimental ones and in line with other *ab initio* calculations. Concerning the bulk modulus, the results with the SZSP basis are worse than those corresponding to the DZSP basis. The calculated magnetic moment for bulk iron ($2.35\mu_B$) is somewhat larger than the experimental value ($2.22\mu_B$), but similar to that of previous all-electron LMTO calculations within atomic sphere approximation (ASA),[48] and to the pseudopotential results quoted in Table II. It is important to stress again the importance of the pseudopotential for this system. For the $[\mathrm{Ar}]3d^6 4s^2$ pseudopotential, the converged magnetic moment is $2.24\mu_B$ for the experimental lattice parameter and $2.28\mu_B$ for the theoretical one. At the level of these calculations, the pseudopotential is more problematic than the basis set.

In order to further check the reliability of our pseudopotential calculation, we performed an *ab initio* tight-binding (TB) LMTO (Ref. 49) study of Fe bulk, using the GGA functional of Perdew and Wang.[38] Not only the magnetic moments are very close (as shown above), but also the density of states is similar, as can be seen in Fig. 1.

C. Fe(100) surface

The loss of coordination at the surface atoms influences the electronic and magnetic properties of the system, as compared with those of the bulk. In order to mimic the Fe(100) surface, we have taken a slab of 13 Fe layers. Checks demonstrated that the results did not change significantly when considering thicker slabs. Previous all-electron *ab initio* studies of the same surface by Ohnishi, Freeman, and Weinert[50] have been performed by means of the FLAPW method[5] for a slab of 7 Fe layers.

We have calculated the electronic and magnetic properties of the Fe(100) surface for SZSP and DZSP basis sets with the same cutoff radius of the pseudo-orbitals used in the bulk and with enough k points in the Brillouin zone to get converged energy and magnetic moments. For the sake of comparison we have also performed a TB-LMTO GGA calculation in the same conditions, that is, a slab of 13 Fe layers. In this TB-LMTO calculation we consider enough empty spheres to avoid the Fe-Fe interaction in different cells. In Table III we present our SIESTA results for SZSP and DZSP basis as compared with our TB-LMTO calculations and also with the all-electron FLAPW results obtained by Onishi, Freeman, and Weinert.[50] For both basis sets (SZSP and DZSP) we obtain an enhancement in the magnetic moment of the surface atoms compared to the bulk. In going from the surface to the central layers, we get a reduction in the magnetic moment until we find nearly the bulk magnetization in the central layer. The magnetic moments obtained with SZSP basis are systematically slightly smaller than those obtained with the DZSP basis.

The magnetic moments obtained are a little larger than with other *ab initio* calculations that use all-electron full-potential methods, but they are smaller than the ones obtained by Weinert, Blügel, and Johnson[51] ($3.77\mu_B$) through a modified valence-only FLAPW method in which the mag-

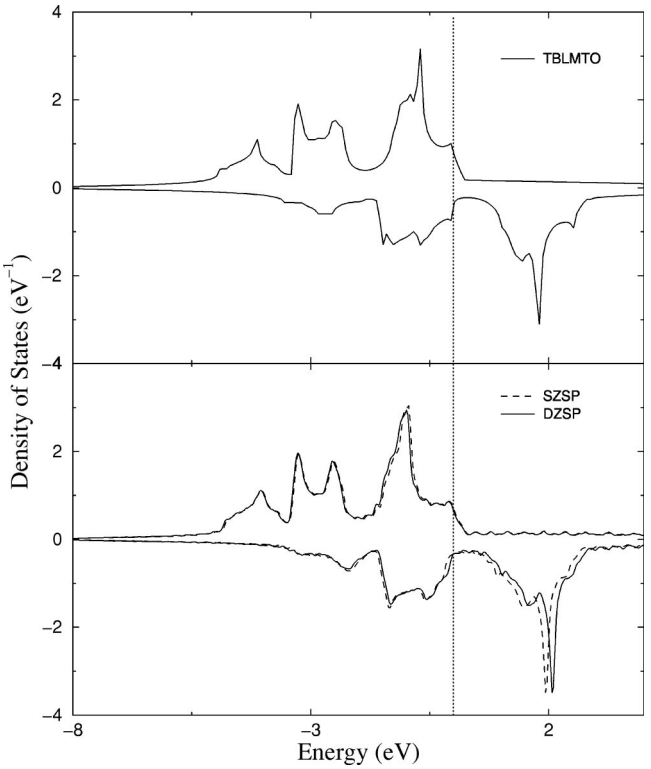

FIG. 1. Total density of states, in eV^{-1} per atom, for the majority and minority spin channels of bulk bcc Fe calculated with the TB-LMTO method (upper panel) and with SIESTA (lower panel) using two different basis sets: double zeta (continuous line) and single zeta (dashed line), both of them including an extra p polarizing orbital.

TABLE III. Local magnetic moments obtained for the Fe(100) surface with SZDP and DZSP basis sets. *S*-*n* represent the different underlayers below the surface (*S*) and *S*-6 corresponds to the center of the slab. Results from other *ab initio* calculations are also presented for the sake of comparison. FLAPW calculations were performed for a slab of seven layers; therefore in this case S-3 is the slab central layer.

	S	$S-1$	$S-2$	$S-3$	$S-4$	$S-5$	$S-6$
SZSP	3.04	2.43	2.50	2.41	2.39	2.37	2.36
DZSP	3.08	2.46	2.52	2.43	2.42	2.40	2.39
TB-LMTO(LDA)	2.92	2.07	2.28	2.18	2.15	2.16	2.12
TB-LMTO(GGA)	2.99	2.13	2.35	2.24	2.20	2.19	2.16
FLAPW [a]	2.98	2.35	2.39	2.25			

[a]Reference 50.

netic contributions are determined by the valence density only. On the other hand, our small overestimation of the magnetic moments is also present in our Fe bulk calculations, but the general trend in going from the surface to the center of the slab (bulk) is correctly described.

Another test of our model is to examine the surface charge density. The fact that we obtain a good agreement for an integrated magnitude like the magnetic moment does not guarantee a good agreement in the spin-density map that reflects the spatial electronic distribution on the surface. This magnitude is available in the study of Onishi, Freeman, and Weinert,[50] and in Fig. 2 we compare it with the corresponding spin density from our DZSP calculation. The agreement between both spin-density contours is quite satisfactory.

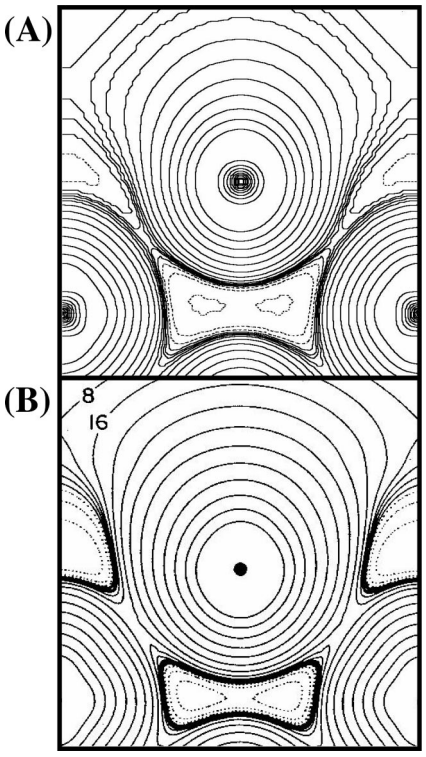

FIG. 2. (a) Self-consistent spin-density map of Fe(100) obtained through a 13-layer calculation within the GGA and a DZSP basis, compared to (b) a seven-layer all electron FLAPW calculation (Ref. 50). Dashed contour lines correspond to negative spin density. Each contour line differs by a factor of 2 in both panels (a) and (b). The contours around the Fe sites in the upper panel (a) are an artifact of the pseudopotential. It is important to remark that due to the scaling, small spin density differences between the two calculations can be magnified in the contour plot.

For completeness we have also calculated with the SIESTA code and with the TB-LMTO GGA method the electronic structure and the magnetization for a (100) free-standing Fe monolayer. The magnetic moments found with the SZSP and DZSP basis sets are $3.19\mu_B$ and $3.23\mu_B$, respectively, and the TB-LMTO result is $3.15\mu_B$. The SIESTA calculation leads to an enhancement of about $0.15\mu_B$ with respect to the (100) surface, due to the loss of coordination.

IV. IRON SYSTEMS SUPPORTED ON Ag(100)

In the previous section we have shown the capability of the method for correctly describing different geometrical environments for pure Fe systems. In this section we test it in mixed systems, where new ingredients are present like interfaces and hybridization effects. We have chosen Fe-Ag systems because Ag is a noble-metal substrate often used in experimental growth processing in order to minimize the interference of the overlayer-to-substrate bonding with the interlayer.

A. Iron monolayer on Ag(100)

We start with the Fe monolayer supported on the fcc Ag(100) substrate. In this example we have to deal not only with the loss of bonds at the surface but also with the interaction between Fe (ferromagnetic) and Ag (noble metal, paramagnetic) that can influence the electronic and magnetic properties of the supported Fe atoms. Previous experimental[52] and first-principles calculations[53,54] have established that Fe and Co monolayers on Ag(100) are ferromagnetically ordered whereas V, Cr, and Mn monolayers on Ag(100) display antiferromagnetic order.

We have first tested bulk Ag to choose the right cutoff radii for the pseudo-orbitals in order to minimize the energy, resulting in a cutoff radius of 5.60 a.u. for all Ag pseudo-orbitals. Then we use this basis set for all Ag calculations.

We construct our system by taking Fe atoms in the pseudomorphic position of fcc Ag and we consider the same lattice parameter for Ag and Fe, like in the previous *ab initio* calculations of Blügel *et al.*,[55] using the FLAPW method, and of Stepanyuk *et al.*,[56] using the KKR Green's-function method.[6]

Results obtained for SZSP and DZSP basis are compared in Table IV with those of two previous *ab initio* calculations.

TABLE IV. Magnetic moments (in units of μ_B) for a free-standing monolayer (FSM) of iron at Ag lattice distance and for a Fe supported monolayer (SM) on Ag(100) calculated with SZSP and DZSP basis sets. FLAPW and KKR calculations for the same systems are also shown for comparison.

	SZSP	DZSP	FLAPW [a]	KKR [b]
FSM	3.35	3.40	3.29	3.30
SM	3.02	3.10	3.01	3.00

[a]Reference 55.
[b]Reference 56.

We can see an enhancement in the magnetic moment of the Fe overlayer due to the loss of bonds. The magnetic moment is slightly lower than for a free-standing Fe monolayer, due to the interaction with the Ag substrate. As in the pure Fe systems, the magnetic moment obtained with DZSP basis is a little bit larger than that obtained with the SZSP, but the trends for both of them are similar and compare very well with the data available from FLAPW and KKR calculations. We obtain also a small charge transfer from iron to Ag ($0.10e^-$ per atom) that is also present in the previous all-electron *ab initio* calculations.

B. Iron clusters on Ag(100)

In this section we study the magnetic behavior of different types of iron clusters on Ag(100). From the experimental point of view, supported clusters are easier to grow and characterize than free-standing clusters. Besides, most of the applications for magnetic devices are based on supported systems.

We have studied a single adatom, one-dimensional (1D) linear wires, planar clusters (2D), and small 3D Fe nanostructures on Ag(100). We have taken fixed positions, so that no relaxations are permitted. The corresponding geometries are shown in Fig. 3, indicating the inequivalent sites. The local magnetic moments of each inequivalent atom are reported in Table V. Our results can be compared with recent KKR calculations by Stepanyuk *et al.*[57] for planar Fe clusters on Ag (adatom and nine-atom cluster). These data are also included in Table V. The atoms displaying larger moments are those located at the corners (the least coordinated ones) and those located in the center have reduced magnetic moment because they have more Fe neighbors. The absolute values of the local moments in our calculations are slightly larger than those obtained by the KKR method (always the DZSP basis gives a little bit larger values than the SZSP basis set). However, the relative difference between the local magnetic moments in different inequivalent sites is nearly the same, so that the effect of the different environments is reflected in the same way for both models and the magnetic trends are correctly described. Also in both methods, KKR and SIESTA, we find a small charge transfer from Fe to Ag, due to the hibridization effects, and the difference between the magnetic moments of the free-standing Fe monolayer at Ag distance and the supported Fe monolayer is nearly the same.

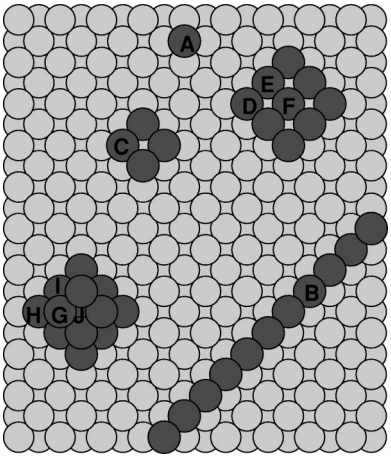

FIG. 3. Labelling of the different inequivalent sites of Fe nanostructures supported on Fe(100) as used in Table V.

For the other supported clusters, atomic wire (only one inequivalent atom), and 3D nanostrutures, the discussion for planar clusters is still valid, local magnetic moments obey the coordination rule.

V. SUMMARY

In this work we have performed *ab initio* pseudopotential calculations of the electronic and magnetic properties of pure and mixed Fe systems with the numerical-LCAO DFT method, using the SIESTA code. We have compared our results with available data obtained through different well-known *ab initio* methods in order to demonstrate the capabilities of ours for describing magnetic systems.

TABLE V. Results for the local magnetic moments (in units of μ_B) at the inequivalent sites of several Fe clusters supported on Ag(100), using SZSP and DZSP basis. The inequivalent sites are indicated with capital letters in Fig. 3. Available KKR data for the adatom and for the nine-atom cluster are given for comparison.

			SZSP	DZSP	KKR [a]
0D	adatom	*A*	3.36	3.47	3.32
1D	wire	*B*	3.17	3.24	
2D	four atom	*C*	3.23	3.33	
	nine atom	*D*	3.26	3.34	3.22
		E	3.23	3.31	3.17
		F	3.17	3.26	3.11
3D	13 atom	*G*	3.15		
		H	3.17		
		I	3.04		
		J	2.91		

[a]Reference 57.

We have constructed the nonlocal pseudopotential of iron from the atomic configuration $[Ar]3d^7 4s^1$ and of silver from $[Kr]4d^{10}5s^1$. In both cases we have used the GGA approximation and nonlinear core corrections. Two different sets of basis have been used: SZSP and DZSP. The cutoff radii for the basis orbitals have been chosen to minimize the energy for bulk bcc Fe and bulk fcc Ag.

We have studied the following systems: Fe dimer, bulk bcc Fe, Fe(100) surface, free-standing Fe monolayer, Fe monolayer on Ag(100), and several Fe clusters supported on Ag(100). The results are in good agreement with the experimental values (when available) and with previous *ab initio* (mainly all-electron) calculations. The method is able, therefore, to deal with complex low-dimensional magnetic systems, taking correctly into account the finite-size effects like reduced coordination and symmetry as well as hybridization effects.

The absolute values for the magnetic moments are sometimes a little bit larger (about $0.15\mu_B$) than in all-electron calculations, and the magnetization obtained using SZSP is slightly smaller than the one obtained with DZSP. For Fe, we find similar trends with SZSP and DZSP basis sets, but the computational cost (CPU and memory) of SZSP calculations is extremely reduced.

In order to compare with previous calculations, we have used fixed atomic positions, so that no relaxations are considered. The SIESTA method, however, allows relaxations and molecular dynamics by calculating the forces on the atoms and the stress tensor from the Hellman-Feynman theorem with Pulay corrections.[12] The computational cost would be obviously higher than with a frozen geometry, but calculations for complex magnetic systems are still feasible and cheaper than with other *ab initio* methods (KKR, FLAPW, LMTO). Also our method does not require the inclusion of empty spheres as it is the case for the LMTO-ASA method. Besides, going from 2D to 3D supported clusters of similar size does not increase the computational cost, like in the KKR method where Green's functions have to be computed. The next step will be to study more realistic, supported, magnetic nanostructures, introducing relaxations and noncollinear magnetization.

ACKNOWLEDGMENTS

We acknowledge financial support of DGICYT of Spain (Grants Nos. PB95-0202 and PB98-0368-C02-01) and of Junta de Castilla y León (Grant No. VA70/99). J.I. acknowledges a F.P.I grant from M.E.C. of Spain. D.S.P. acknowledges support from Grants Nos. DOE 8371494 and DEFG 02/96/ER 45439. P.O. is the recipient of Sponsored Research Projects from Motorola PSRL and Sumitomo Chemical. P.O. and E.A. acknowledge support of the Ψ_k network of the ESF.

[1] Phys. Today, **48** (4) (1995) special issue on magnetoelectronics.
[2] J. P. Bucher, D. C. Douglas, and L. A. Bloomfield, Phys. Rev. Lett. **66**, 3052 (1991); I. M. L. Billas, A. Chatelain, and W. A. de Heer, Science **265**, 1682 (1994).
[3] A. J. Cox, J. G. Lourderback, S. E. Apsel, and L. A. Bloomfield, Phys. Rev. B **49**, 12 295 (1994).
[4] P. Grünberg, R. Schreiber, P. Yang, M. B. Brodsky, and H. Sowers, Phys. Rev. Lett. **57**, 2442 (1986).
[5] E. Wimmer, H. Krakauer, M. Weinert, and A. J. Freeman, Phys. Rev. B **24**, 864 (1981).
[6] K. Wildberger, V. S. Stepanyuk, P. Lang, R. Zeller, and P. H. Dederich, Phys. Rev. Lett. **75**, 509 (1995).
[7] O. K. Andersen, Phys. Rev. B **12**, 3060 (1975).
[8] See, e.g., M. Payne, M. Teter, D. Allan, T. Arias, and J. D. Joannopoulos, Rev. Mod. Phys. **64**, 1045 (1992).
[9] A. Vega, J. Dorantes-Davila, L. C. Balbás, and G. M. Pastor, Phys. Rev. B **47**, 4742 (1993).
[10] J. Izquierdo, A. Vega, and L. C. Balbás, Phys. Rev. B **55**, 445 (1997), and references therein.
[11] A. Vega, L. C. Balbás, H. Nait-Laziz, C. Demangeat, and H. Dreyssé, Phys. Rev. B **48**, 985 (1993).
[12] P. Ordejón, E. Artacho, and J. M. Soler, Phys. Rev. B **53**, R10441 (1996).
[13] P. Ordejón, E. Artacho, and J. M. Soler, in *Materials Theory, Simulations, and Parallel Algorithms*, edited by E. Kaxiras *et al.*, MRS Symposia Proceedings No. 408 (Materials Research Society, Pittsburgh, 1996), p. 85.
[14] D. Sánchez-Portal, P. Ordejón, E. Artacho, and J. M. Soler, Int. J. Quantum Chem. **65**, 453 (1997).
[15] E. Artacho, D. Sánchez-Portal, P. Ordejón, A. García, and J. M. Soler, Phys. Status Solidi B **215**, 809 (1999).
[16] P. Ordejón, Physica Status Solidi B **217**, 335 (2000).
[17] W. Kohn and L. J. Sham, Phys. Rev. A **140**, A1133 (1965).
[18] J. P. Perdew and A. Zunger, Phys. Rev. B **23**, 5048 (1980).
[19] J. P. Perdew, K. Burke, and M. Ernzerhof, Phys. Rev. Lett. **77**, 3865 (1996).
[20] N. Troullier and J. L. Martins, Phys. Rev. B **43**, 1993 (1991).
[21] L. Kleinman and D. M. Bylander, Phys. Rev. Lett. **48**, 1425 (1982).
[22] T. Oda, A. Pasquarello, and R. Car, Phys. Rev. Lett. **80**, 3622 (1998).
[23] S. G. Louie, S. Froyen, and M. L. Cohen, Phys. Rev. B **26**, 1738 (1982).
[24] S. Huzinaga, *Gaussian Basis Sets for Molecular Calculations* (Elsevier, New York, 1984); R. Poirier, R. Kari, and R. Csizmadia, *Handbook of Gaussian Basis Sets* (Elsevier, New York, 1985), and references therein.
[25] G. L. Zhao, D. Bagayoko, and T. D. Williams, Phys. Rev. B **60**, 1563 (1999).
[26] O. F. Sankey and D. J. Niklewski, Phys. Rev. B **40**, 3979 (1989).
[27] For reviews see P. Ordejón, Comput. Mater. Sci. **12**, 157 (1998); S. Goedecker, Rev. Mod. Phys. **71**, 1085 (1999).
[28] J. A. White and D. M. Bird, Phys. Rev. B **50**, 4954 (1994).
[29] W. H. Press, S. A. Teulosky, W. T. Vetterling, and B. P. Flannery, *Numerical Recipes. The Art of Scientific Computing* (Cambridge University Press, Cambridge, 1992).
[30] D. Vanderbilt, Phys. Rev. B **41**, 7892 (1990).
[31] M. Castro and D. R. Salahub, Phys. Rev. B **49**, 11 842 (1994).
[32] P. A. Montano and G. K. Shenoy, Solid State Commun. **35**, 53 (1980).

[33] H. Purdum, P. A. Montano, G. K. Shenoy, and T. Morrison, Phys. Rev. B **25**, 4412 (1982).
[34] H. Lian, C.-X. Su, and P. B. Armentrout, J. Chem. Phys. **97**, 4072 (1992).
[35] M. Moskovits, D. P. DiLella, and W. Limm, J. Chem. Phys. **80**, 626 (1984).
[36] M. Moskovits and D. P. DiLella, J. Chem. Phys. **73**, 4917 (1980).
[37] S. H. Vosko, L. Wilk, and M. Nusair, Can. J. Phys. **58**, 1200 (1980).
[38] J. P. Perdew and Y. Wang, Phys. Rev. B **33**, 8800 (1986).
[39] P. Söderling, Ph D. thesis, Upsala University, 1994.
[40] P. Bagno, O. Jepsen, and O. Gunnarson, Phys. Rev. B **40**, 1997 (1989).
[41] B. Barbiellini, E. G. Moroni, and T. Jarlborg, J. Phys.: Condens. Matter **2**, 7597 (1990).
[42] T. C. Leung, C. T. Chan, and B. N. Harmon, Phys. Rev. B **44**, 2923 (1991).
[43] D. J. Singh, W. E. Pickett, and H. Krakauer, Phys. Rev. B **43**, 11 628 (1991).
[44] J. Zhu, X. W. Wang, and S. G. Louie, Phys. Rev. B **45**, 8887 (1992).
[45] J-H. Cho, and M. Scheffler, Phys. Rev. B **53**, 10 685 (1996).
[46] C. Kittel, *Introduction to Solid State Physics*, 6th ed. (Wiley, New York, 1986).
[47] J. P. Perdew, in *Electronic Structure of Solids '91*, edited by P. Ziesche and H. Eschrig (Akademie-Verlag, Berlin, 1991).
[48] J. Häglund, Phys. Rev. B **47**, 566 (1993); T. Asada and K. Terakura, *ibid.* **46**, 13 599 (1992).
[49] H. L. Skriver, *The LMTO Method* (Springer, Berlin, 1984); O. K. Andersen and O. Jepsen, Phys. Rev. Lett. **53**, 2571 (1984); O. K. Andersen, Z. Pawlowska, and O. Jepsen, Phys. Rev. B **34**, 5253 (1986).
[50] S. Ohnishi, A. J. Freeman, and M. Weinert, Phys. Rev. B **28**, 6741 (1983).
[51] M. Weinert, S. Blügel, and P. D. Johnson, Phys. Rev. Lett. **71**, 4097 (1993).
[52] J. E. Ortega and F. J. Himpsel, Phys. Rev. B **47**, 16 441 (1993).
[53] Ch. Li, A. J. Freeman, H. J. F. Jansen, and C. L. Fu, Phys. Rev. B **42**, 5433 (1990).
[54] S. Blügel and P. H. Dederichs, Europhys. Lett. **9**, 597 (1989).
[55] S. Blügel, B. Drittler, R. Zeller, and P. H. Dederichs, Appl. Phys. A: Solids Surf. **49**, 547 (1989).
[56] V. S. Stepanyuk, W. Hergert, P. Rennert, K. Wildberger, R. Zeller, and P. H. Dederichs, Phys. Rev. B **54**, 14 121 (1996).
[57] V. S. Stepanyuk, W. Hergert, P. Rennert, K. Wildberger, R. Zeller, and P. H. Dederichs, Phys. Rev. B **59**, 1681 (1999); P. Rennert, V. S. Stepanyuk, W. Hergert, J. Izquierdo, A. Vega, and L.C. Balbás, in *Advances in Science and Thechnology*, edited by P. Vincencini and S. Valeri, Techna Srl, Florence, Italy, 1999), Vol. 19, pp. 29–36.